Effect of residual stress on the optical properties of CdI_2 films

Pankaj Tyagi[1,*] and A. G. Vedeshwar[1,†]
[1]*Thin Film Lab, Department of Physics & Astrophysics, University of Delhi, Delhi - 110 007, India*
(Received 29 November 2001; revised manuscript received 26 March 2002; published 29 August 2002)

The optical absorption near the fundamental absorption edge was measured as a function of film thickness, substrate temperature, and heat treatment temperature for hexagonally structured (4H polytype) stoichiometric CdI_2 films. The structural analysis shows a well oriented (hh0) parallel to substrate plane with residual tensile stress in the film. Residual stress was found to increase nonlinearly with both film thickness and treatment temperature while it decreases linearly with substrate temperature. The optical absorption analysis shows both direct and indirect types of interband transitions in agreement with earlier studies. The combined data from all the three dependences show the existence of a threshold residual tensile stress (970 atm or 1000 kg/cm^2) above which E_g decreases (5 meV/atm) and grain size increases (0.067 μm/atm) linearly with stress.

DOI: 10.1103/PhysRevB.66.075422 PACS number(s): 68.55.Jk, 78.20.Ci, 81.15.Ef, 78.66.Li

I. INTRODUCTION

Cadmium iodide is an interesting material due to its layered structure having a hexagonal unit cell, which is isostructural with many halides and MX_2-type dichalcogenides.[1] An infinite hexagonal sheet of Cd atoms sandwiched between two similar sheets of I atoms (the Cd atoms being octahedrally coordinated) constitute the basic layer, and such layers are stacked along the third direction to form a three-dimensional compound. The possibility of different stacking sequences due to the weak bonding (van der Waal's) between the layers leads to polytype structures. CdI_2 is a well-known polytype material having a number of polytypes as high as 200, out of which only very few are commonly occurring.[2] Optical studies carried out on single-crystal samples show both direct (by reflectivity[3]) and indirect (by absorption[3–5]) types of interband transitions at 3.8 and 3.2 eV, respectively. The band-structure calculations also reveal the presence of a direct band gap and a slightly smaller indirect band gap differing by about 0.3–0.6 eV.[6–10] However, the studies are quite limited regarding its basic thin-film properties (structural[11,12] and optical[13–16]). The thin films of any material grown by many techniques normally contain remnant or residual internal stress developed during the condensation on the substrate. Internal stress could also affect the physical properties similar to externally applied stress. The thin-film form, therefore, can be an advantageous and convenient system to study such effect, if any. No such studies on pressure dependence, either external or internal, are reported in the literature for CdI_2. Therefore, we systematically studied the film thickness dependence, the effect of the substrate temperature, the effect of heat treatment, etc., on the physical properties of thermally evaporated CdI_2 films.

II. EXPERIMENTAL DETAILS

Films of CdI_2 were grown on glass substrates at room temperature or elevated temperature by thermal evaporation at a vacuum of about 10^{-6} Torr using a molybdenum boat. The starting material was high-purity stoichiometric powder, which was pelletized for evaporation. Substrate temperature was maintained at the desired value with an accuracy of $\pm 5\,^{\circ}C$ during the film growth as measured by a thermocouple placed on the substrate. The film thickness was monitored by a quartz crystal thickness monitor during evaporation and subsequently confirmed by DEKTAK IIA surface profiler measurements. In the present study the deposition rate was kept quite low (0.5–1 nm/s) because the very high deposition rate (>6 nm/sec) led to nonuniform film growth and low sticking. We have shown earlier[17] that the intermediate deposition rate (2–5 nm/sec) leads to *c*-axis modulation with thickness, which may be ascribed to the polytypism of CdI_2. All the films were uniform and transparent. However, very thick films become slightly translucent. The films thicker than 600 nm crack and peel off the substrate, and thinner ones (<30 nm) show a discontinuity with the island structure. We have used only uniform and well-adhered films. Small pieces of 5×5 mm^2 were cut from the uniform portion for carrying out various analyses on the same film. All the films were grown at room temperature (300 K) for studying the effect of film thickness. For studying the effect of heat treatment, films of the same thickness were grown at room temperature and then were heat treated at various desired temperatures. The films were heat treated in air for a very short-time duration (30–40 sec) by placing them on a preheated copper block at the desired temperatures. The film thickness was kept constant within an error of ± 5 nm in all the experiments concerning the effect of heat treatment (360 nm) and substrate temperatures (60 nm). A structural study of the films was carried out by x-ray-diffraction analysis (PHILIPS X-Pert model PW-1830 generator diffractometer). The film composition of the as grown films was found to be stoichiometric as determined by EDAX (JEOL - 840). However, no noticeable deviation from stoichiometric film composition was observed for heat-treated films or films grown at substrate temperatures up to 200 °C. The morphology of the film was studied by scanning electron microscopy (SEM) (JEOL - 840). The optical absorption measurements were carried out in ultraviolet/VIS region using a (Shimadzu UV - 260) spectrophotometer. All the measurements concerning various analyses were carried out at room temperature (300 K) in this study.

III. RESULTS AND DISCUSSION

All the films grown either at room temperature or at an elevated substrate temperature up to 200 °C were completely polycrystalline and stoichiometric (from x-ray diffraction and EDAX analysis) without any exception. However, an earlier report[12] on an structure of CdI_2 films showed that films thinner than 100 nm were amorphous and that thicker films tended to crystallize. It is also known that CdI_2 films grown at a substrate temperature of less than 300 K are amorphous and that those either grown or annealed above 300K are polycrystalline.[18] X-ray diffraction analyses of all the films show a high degree of crystallite orientation with (hh0) parallel to substrate plane indicated by the major peaks observed from (110), (220), (330), and (440) reflections. There were few other peaks of negligible relative intensity ($<2\%$) from (001), (101), or (111) reflections. Earlier studies[11,12] have also observed this kind of crystallite alignment in CdI_2 films. Our x-ray-diffraction data agree very well with the earlier report[11] as well as ASTM No.(12-574). The structural polytype of our films can be identified as 4H from the cell dimensions. The x-ray-diffraction data can also be used to determine internal stress in the sample. The displacement of diffraction peaks from their corresponding stress-free data indicates a uniform stress developed normal to the corresponding crystal plane in the film during condensation. If the diffraction peaks shift to lower angle (increasing d), a tensile stress can be realized. Similarly, the decrease in d indicates a compressive stress. The nonuniform stress is indicated by an increase in full width at half maxima of the diffraction peak.[19,20] All major peaks from (hh0) observed in our x-ray data show a slight displacement toward lower angle as compared to powder data (ASTM No. 12-574). We have illustrated this fact in Fig. 1 for the strongest peak (110). The magnitude of shift varies slightly from peak to peak. Therefore, we have taken the average of strain

$$\frac{\Delta d}{d} = \frac{d(\text{Observed}) - d(\text{ASTM})}{d(\text{ASTM})}$$

for all four peaks. The residual stress in the film can be determined by multiplying $\Delta d/d$ by the elastic constant of the material. Therefore, we can call $\Delta d/d$ the residual stress parameter. By the geometry of x-ray diffraction, the observed peaks are from crystal planes parallel to the substrate plane. The increased d spacing of these planes as observed in the present study indicates a tensile stress normal to the planes. We have thus determined the average $\Delta d/d$ for dependences of treatment temperature, film thickness and substrate temperature as shown in Fig. 2. We can see an almost similar behavior for the effect of the film thickness and treatment temperature, while the trend is quite opposite in the case of the effect of substrate temperature.

Almost all the films grown by any technique normally have a residual stress of the magnitude that depends on the material and growth conditions. In a film residual stress may occur at the scale of microstructure (intergranular microstress) as well as at the level of crystal structure (intragranular microstress). Such stresses are, by necessity, balanced by stresses in other locations (or directions) or crystal planes

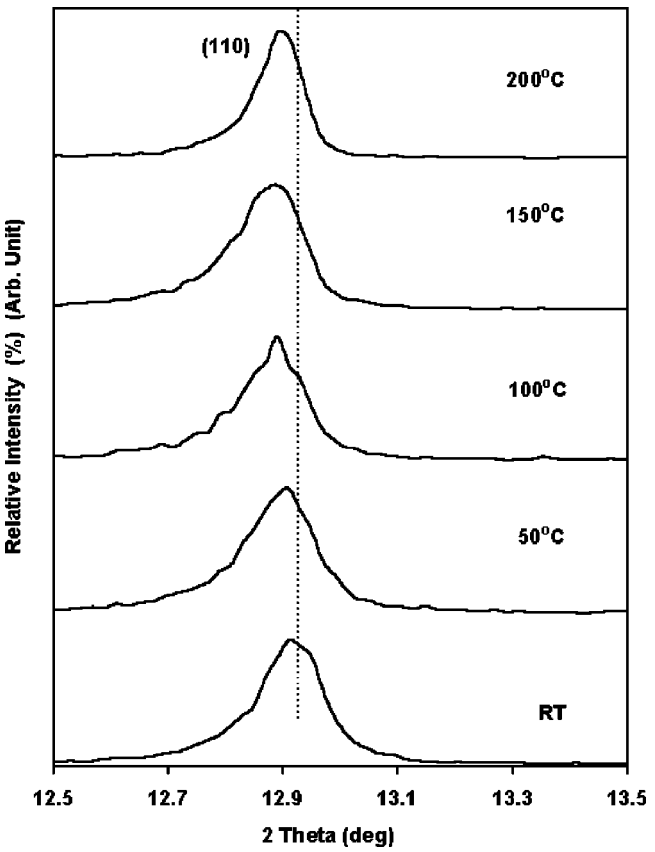

FIG. 1. Shifting of the (110) peak position from corresponding powder data ASTM No.12-574 (the vertical broken line) resulting in the increase of d_{110} of CdI_2 films heat treated at various temperatures (identified in the figure).

within the material for an equilibrium configuration.[21] X-ray-diffraction data can determine the residual stress only at the level of crystal structure. The intergranular microstress can be determined by optical interferometric methods. Both measurements on same sample can rarely be found. In this context, the tensile stress along the thickness as determined by the x-ray data of the present study must be balanced by some other stresses for equilibrium. It may be noted that the balancing stress could be of the same type (tensile) in the perpendicular direction or of the opposite type (compressive) in the same direction. The first possibility—that is, the tensile stress normal to film thickness or along the length of the film—seems to be relevant and operative in the present study. The optical interferometric method measures the stress along the film length,[22] and such a measurement has revealed a tensile stress in similar halide films[23] such as MgF_2, $ThoF_2$, PbF_2, CeF_3, etc. The tensile stress along the film length could be both intragranular and intergranular. However, the intragranular nature along film length cannot be analyzed by the present x-ray-diffraction (XRD) data. The intergranular stress is usually measured by optical interferometry which was not possible in the present study. We can assume a dominating intergranular microstress along film length similar to that observed in few similar halide films,[23] as mentioned above. Therefore, an intergranular tensile stress along film length could well exist. Further, this fact is also

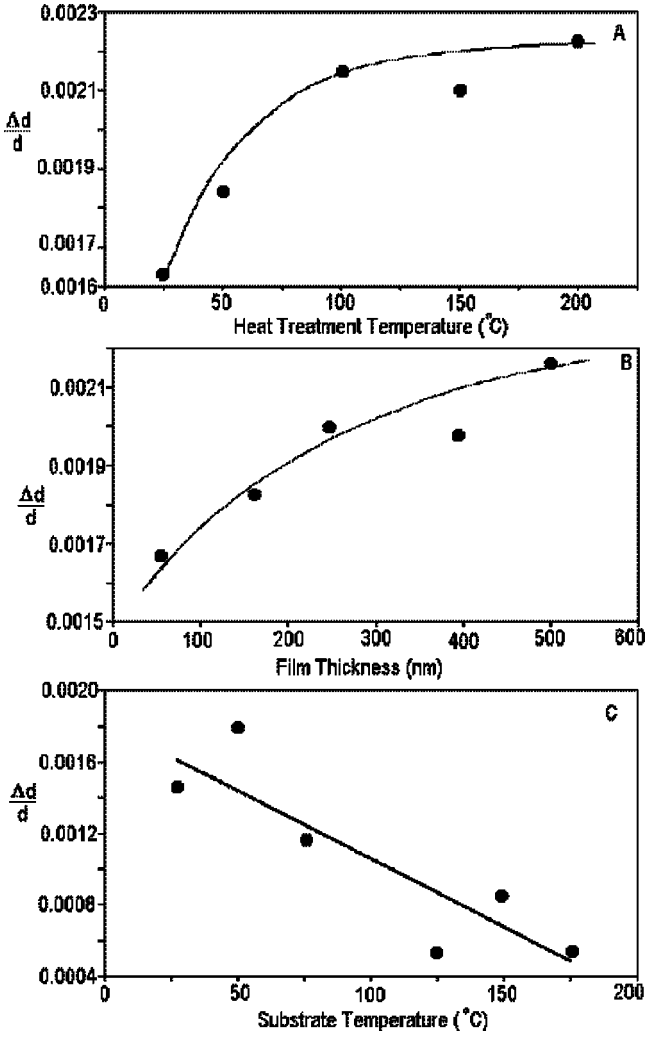

FIG. 2. Dependence of residual tensile stress parameter $\Delta d/d$ on (A) heat treatment temperatures (360-nm-thick film grown at room temperature and then treated at desired temperatures), (B) film thickness (grown at room temperature), and (C) substrate temperatures (60-nm-thick films) for CdI_2 films.

revealed by SEM analysis, as displayed in Fig. 3. We have shown a few representative SEM photographs in Fig. 3 for all three dependences. The grains grow in size along the film length, and become flattened with both film thickness and treatment temperature. The opposite behavior can be seen for effect of substrate temperature consistent with the residual stress behavior. Therefore, we strongly believe that the tensile stress along the thickness (as determined by XRD) must be balanced by the intergranular tensile stress along the film length.

The thickness dependence of the residual stress may simply reveal the growth stress (σ_I) or internal stress developed during deposition when film deposition and stress measurements are made at the same temperature. However, the residual stress will be altered when film deposition occurs at temperatures different from that at which stress is measured. This happens mainly due to the difference in the thermal expansion coefficient of film and substrate. The development of stress due to this is normally called thermal stress, $\sigma_f(T)$, which superimposes on the growth stress giving the total residual stress in the film as[22] $\sigma_f = \sigma_f(T) + \sigma_I$. The thermal stress is given by[22]

$$\sigma_f(T) = (\alpha_s - \alpha_f)\Delta T E_f/(1-\nu_f), \tag{1}$$

where α_s and α_f are the coefficients of the linear thermal expansions of the substrate and film, respectively; ΔT is the temperature difference; E_f is the Young's modulus of the film; and ν_f is the Poisson ratio of the film. In this context, the behaviors of the residual stress with the treatment temperature and substrate temperature would be of similar natures showing a monotonic increase. However, it should be noted that there is difference in the two processes. In our heat-treatment experiment samples were heat treated only for few seconds in air, and therefore the process can be assumed similar to quenching. In this case the development and superimposition of thermal stress on growth stress can be expected, as predicted by Eq. (1). The derivation of Eq. (1) is based on a linear expansion along the film length, and predicts the stress in the same direction. As we discussed above, the increased intergranular microstress along the film length in the process causes an increase in the stress along the film thickness as observed in Fig. 2(A) as a function of the treatment temperature. In the case of an elevated substrate temperature, the cooling takes place very slowly (a few hours) due to the vacuum and is equivalent to annealing. In addition, the growth process itself will be affected by the elevated substrate temperature. Therefore, heated substrates alter the intrinsic stresses largely by promoting defect annealing and the process of recrystallization. The resultant softening relaxes the growth stresses, which fall rapidly with temperature.[22] We can see that the magnitude as well as behavior of $\Delta d/d$ are quite consistent with the above idea as far as substrate temperature is concerned, as seen in Fig. 2(C). We may add the fact that the film cracks above the upper limits of both film thickness and treatment temperature shown in Figs. 2(A) and 2(B). This may show the ever increasing intergranular stress and the cracking or breaking when an imbalance between along the thickness and along the length stresses develops. We have plotted the average grain size as a function of $\Delta d/d$ in Fig. 4 (results of all three experiments) to see explicitly the dependence of grain growth on intergranular microstress. Of course, it is assumed that the measured $\Delta d/d$ along the thickness is equal to the microstress along the length since the film is in equilibrium. We can note the existence of a threshold stress $\Delta d/d = 0.0019$ above which the grain size increases linearly with stress. It is quite difficult to reason out this behavior at this stage.

We have carried out optical absorption/transmission measurements on all the samples which were structurally and morphologically well characterized. Some representative optical absorption data as a function of wavelength are shown for a heat-treated 360-nm-thick film at different temperatures in Fig. 5. The absorption coefficient α was calculated by the measured absorption A as a function of incident photon wavelength using a relation

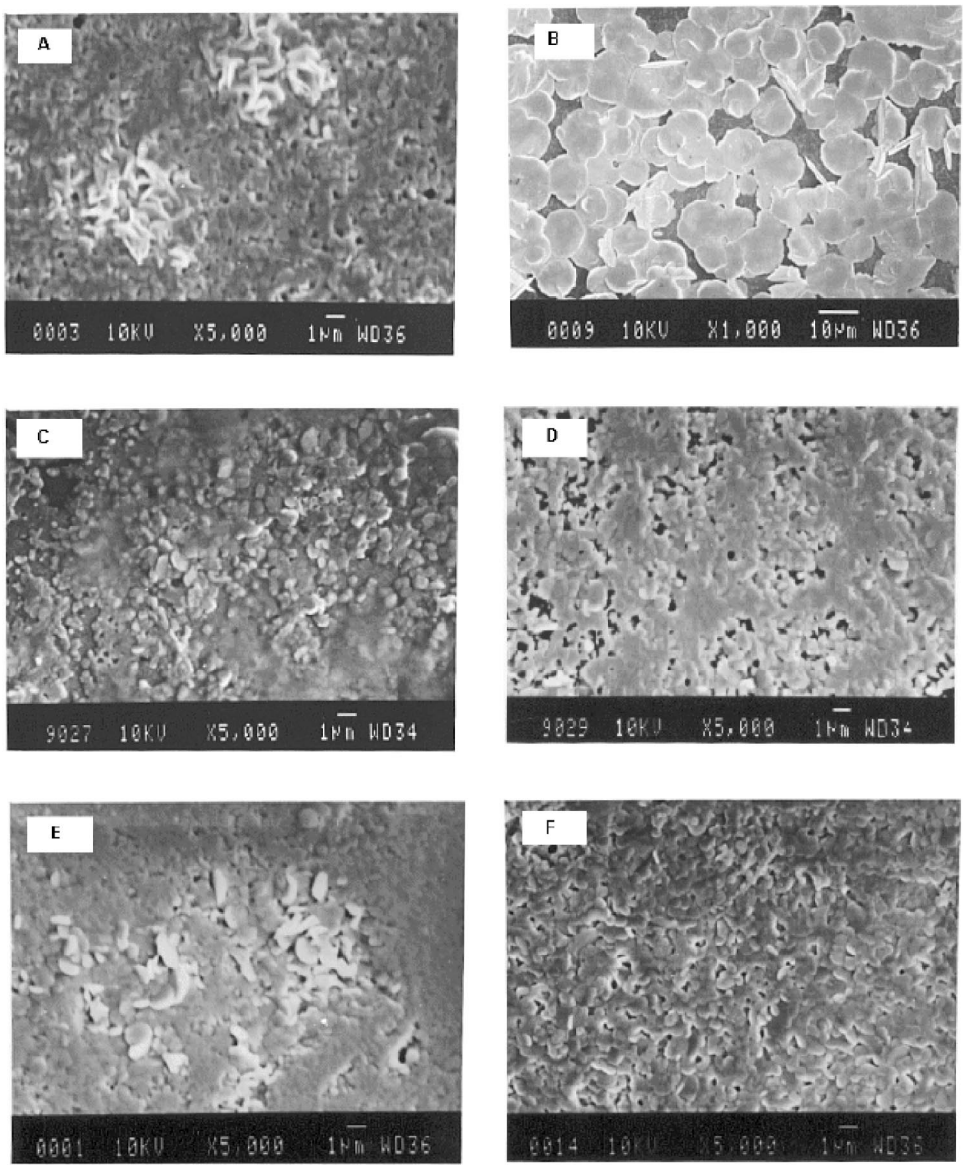

FIG. 3. SEM micrographs showing the crystallite morphology of CdI_2 films (grown at room temperature) treated at (A) 50 °C and (B) 200 °C. Similarly, (C) and (D) show the morphology of as-grown 55- and 500-nm-thick films at room temperature, respectively. (E) and (F) are for films grown at substrate temperatures of 50 and 125 °C, respectively.

$$\alpha = \frac{2.303A}{t}, \tag{2}$$

where t is the film thickness, neglecting the reflection coefficient, which is insignificant near the absorption edge. The wavy nature of the absorption away from the fundamental absorption edge is due to the interference fringes arising from the substrate-film and film-air interfaces. It can be seen from the figure that these fringes smoothe out as the treatment temperature increases. The fringe pattern is much more pronounced in transmission spectra and will be utilized to determine the refractive index (n) as a function of wavelength. The steep rise in the absorption coefficient near the absorption edge hints at a direct type of transition. In a polycrystalline material the nature of optical interband transitions (direct or indirect) near the absorption edge can be determined by the relation between α and the optical energy gap E_g. Assuming parabolic bands, the relation between α and E_g for a direct transition is given by[24]

$$\alpha h\nu = \text{const}(h\nu - E_g)^n, \tag{3}$$

and for indirect transition by[24]

$$\alpha h\nu = \frac{A(h\nu - E_g + E_p)^n}{\exp(\theta_D/T) - 1} + \frac{B(h\nu - E_g - E_p)^n}{1 - \exp(-\theta_D/T)} \tag{4}$$

where E_p is the phonon energy assisting the transition, θ_D is the Debye temperature, and A, and B are constants. For a direct transition $n = 1/2$ or $3/2$ depending on whether the transition is allowed or forbidden in quantum mechanical sense. Similarly, $n = 2$ or 3 for indirect allowed and forbidden transitions, respectively. The usual method of determining the energy gap is to plot $(\alpha h\nu)^{1/n}$ against $h\nu$ and look for that value of n which gives the best linear graph in the absorption edge region. Obviously, there will be a single linear region in the case of a direct transition and two linear portions for an indirect transition as can be seen from Eqs. (3) and (4). We have plotted $(\alpha h\nu)^{1/n}$ versus $h\nu$ for CdI_2

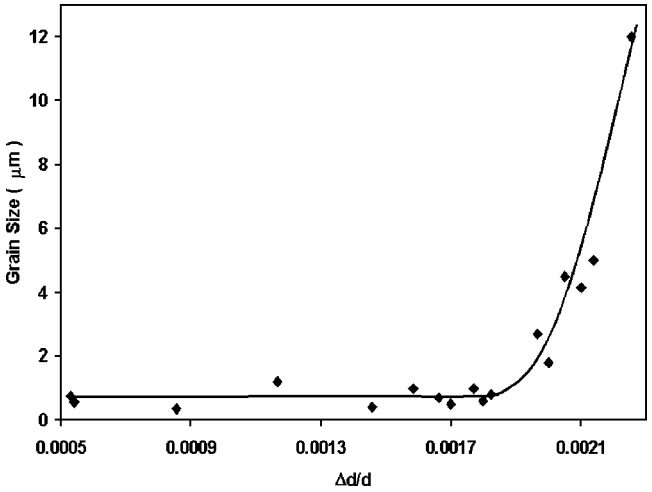

FIG. 4. Growth of grain size with residual tensile stress parameter $\Delta d/d$ in CdI_2 films.

films treated at different temperatures, and the best fit was obtained for $n=1/2$ indicating a direct allowed transition as shown in the inset of Fig. 5.

In earlier reports[3,4] the absorption data on single crystals were fitted to $n=2$ to obtain an indirect gap of 3.2 eV by the plot of $(\alpha)^{1/2}$ versus $h\nu$. However, in Ref. 4 authors clearly indicate that the data fit equally well with $n=3$ and the exact nature of the transition is not certain. Using the data of α versus $h\nu$ in Refs. 3 and 4, we have found that the best fit is obtained for $n=1/2$, that is a direct transition. A peak corresponding to a direct band-to-band transition has been identified in the reflectivity spectra at 3.8 eV (at room temperature)[3] and at 4.3 eV (at 30 K).[10] We can see that at room temperature both these reports agree very well when we apply the linear temperature coefficient of the energy gap[3] (-1.2×10^{-3} eV/K) to Ref. 10. A direct transition from valence-band maxima to conduction-band minima at 4.1 eV has been determined from electron-energy-loss spectroscopy.[11] The energy-band structure calculations[6–11] clearly show the existence of both direct and indirect band gaps of similar magnitudes; the difference between the two is about 0.3–0.6 eV. However, the band structure[9] and band gaps[25] of CdI_2 are shown to be insensitive to its polytypes. Therefore, we can realize that both indirect and direct band gaps exist in CdI_2, and are separated by just 0.3–0.6 eV. Since the indirect gap is just less than the direct gap, it lies near the onset of direct gap and can hardly be noticed in the $(\alpha h\nu)^2$ versus $h\nu$ plot of much dominated direct transition. Therefore, the part of the optical absorption data near the knee or tail of the direct absorption edge have to be replotted as $(\alpha h\nu)^{1/2}$ versus $h\nu$ to determine the indirect gap. The details of such an analysis were reported earlier[17] by us and therefore are not shown here. The value of the indirect energy gap also agrees quite well with those in the literature. However, we still believe that the optical absorption data clearly reveal a direct energy gap showing the best fit to $n=1/2$. Thus the determined value of E_g (indirect) agrees well with earlier experimental results as well as band-structure calculations. Our value of E_g (direct) of 3.6 eV determined

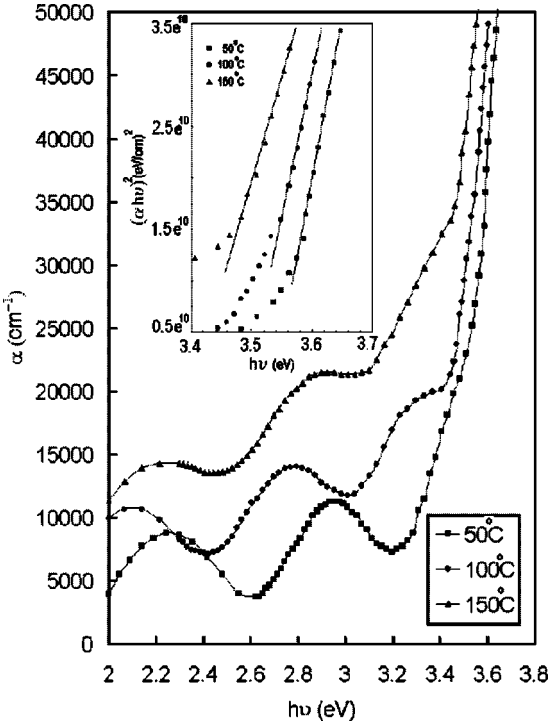

FIG. 5. Optical absorption coefficient α as a function of incident photon energy for three heat-treated 360-nm-thick CdI_2 films. The treatment temperature are indicated in the figure. The inset shows the plot of $(\alpha h\nu)^2$ vs $h\nu$ for determining the direct optical energy gap by the extrapolation of the linear part (shown by straight lines).

for films of thickness $\leqslant 250$ nm agrees well with the predicted value 3.8 eV from band-structure calculations. We will consider only a direct optical energy gap in this paper. The direct optical energy gap (E_g) so determined varies more systematically with film thickness and treatment temperature than with substrate temperature, as shown in Fig. 6. The variation in E_g with these parameters could be due to various reasons. For example, the variation of E_g with film thickness can be ascribed to the quantum size effect if the film thickness is too small compared to the mean free path or to changing grain boundary barrier heights, especially in doped semiconductors, or to the defect density in the film. However, none of these seems to be relevant or effective in the present material. The exact dependence of the defect density is almost impossible to establish from the present study. Since we have seen some systematic behavior of residual stress with these parameters, we can try to see some correlation between residual stress and E_g. Generally, the effect of externally applied pressure or stress (compressive) is well known in many materials because of fractional changes in atomic positions due to strain, which would modify the band structure slightly. The effect of an externally applied tensile stress is rarely known. We plot E_g as a function of $\Delta d/d$ in Fig. 7, combining all the data from Figs. 2 and 6. We see that E_g is almost independent of $\Delta d/d$ up to 0.002 and then decreases linearly with $\Delta d/d$. Therefore, we can say that there exists a threshold tensile stress above which E_g decreases linearly. The elastic constant $C_{11}=0.491\times10^{11}$ N/m^2 for a CdI_2 single crystal.[26] The diagonal elements of the elastic matrix

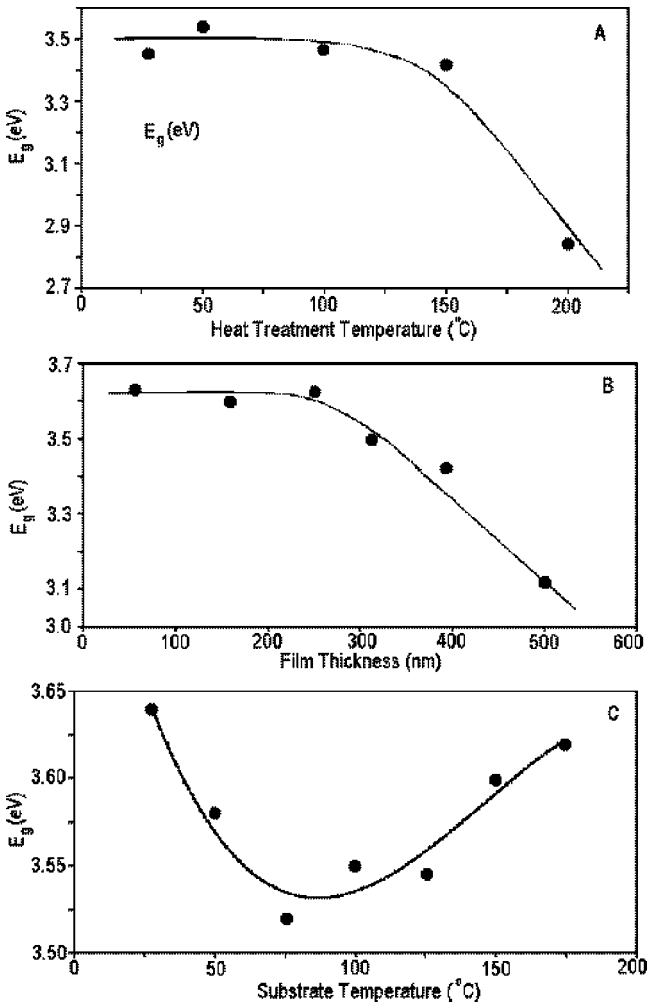

FIG. 6. The variation of E_g with (A) treatment temperatures (the film grown at room temperature was treated at desired temperature), (B) film thickness (grown at room temperature), and (C) substrate temperatures for CdI_2 films. E_g was determined for the samples used in Fig. 2.

are the principal elastic constants representing pure tensile or compressive components, and the off-diagonal terms represent shear components. In all the concerned figures we have represented the stress by $\Delta d/d$ to differentiate it from directly measured or externally applied stress. The threshold stress can be calculated using the elastic constant as 9.8×10^7 N/m^2 (970 atm or 1000 kg/cm^2). However, it should be noted that C_{11} is not the exact component along the [110] direction and we have used it only for the purpose of estimating the order of magnitude of the stress here. Incidentally, the order of magnitude of the tensile stress (along thickness by XRD), determined roughly here, matches quite well with those (intergranular microstress along film length determined by optical interferometry) observed for some similar halides like PbI_2, CeF_3, MgF_2, and $ThOF_2$ films[23] for which stress analysis by XRD is not available. Therefore, we strongly believe that the tensile stress along the thickness as detected by XRD here must develop in accordance with the intergranular tensile stress along the length for the purpose of balance or equilibrium up to a certain limit beyond which the

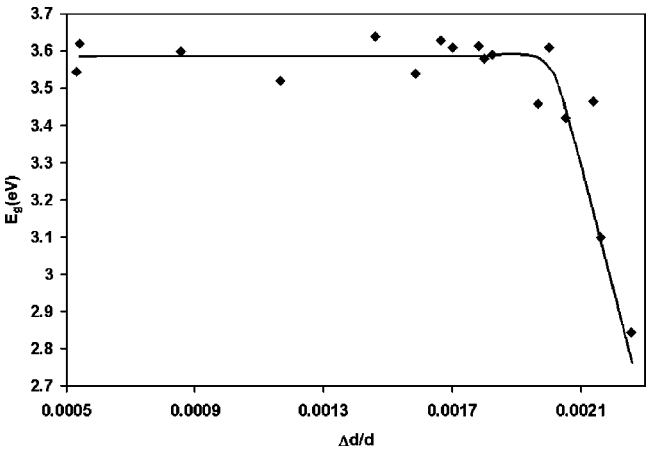

FIG. 7. The variation of E_g with the residual stress parameter $\Delta d/d$ for combined data from all three experiments.

film breaks due to excesive tensile stress along the length. Above the threshold stress E_g decreases linearly with stress at a rate of 5 meV/atm. In an earlier study[27] on the hydrostatic pressure effects on optical excitations of lead and cadmium halides in the range 1000–3500 atm a linear increase of 5.5 μeV/atm was observed for CdI_2 film for an optical edge at 4 eV. In contrast to this a linearly decreasing trend was observed for PbI_2 film. It should be noted that the stress was an overall compressive one on the sample as opposed to the tensile stress on the (110) orientation of the present study. The cross section of (110) of the 4H-type structure of CdI_2 contains five Cd atoms on the plane surrounded by two I atoms on either side of the plane. Increasing d_{110} means an increase in I-I distance. In electronic structure calculations of cadmium halides[10] the calculated and experimental band gaps decrease with increasing anion-anion distance from $CdCl_2$ to CdI_2. However, the exact modification or change in the band structure due to the fractional change in I-I distance is hard to find. We strongly feel that the observed large decrease of 5 meV/atm is mainly due to the modification of the valence band arising from I $5p$ character due to the increasing I-I distance resulting from the tensile stress perpendicular to (110). The effect of intergranular microstress along film length may not be significant or substantial on the band gap because the increase in the c parameter (polytypism) along the length in this oriented film is insensitive to the band gap, as mentioned earlier.

As mentioned earlier, the interference fringes observed in the transmission spectra can be used to determine optical constants of the material like the refractive index (n), absorption index (k), etc., by drawing the envelope on the maxima and minima of the fringe pattern in the transmission spectrum. The detailed description of the procedure is given in Ref. 28. In this method the accuracy of determining n is very good in the region quite away from absorption edge. The accuracy crucially depends upon the envelopes on the fringe pattern. Near the absorption edge the distance between the two envelopes decreases and the error in determining these can cause a significant inaccuracy of n in this region. Therefore, the refractive index data determined by this method near the absorption edge may not be quite reliable.

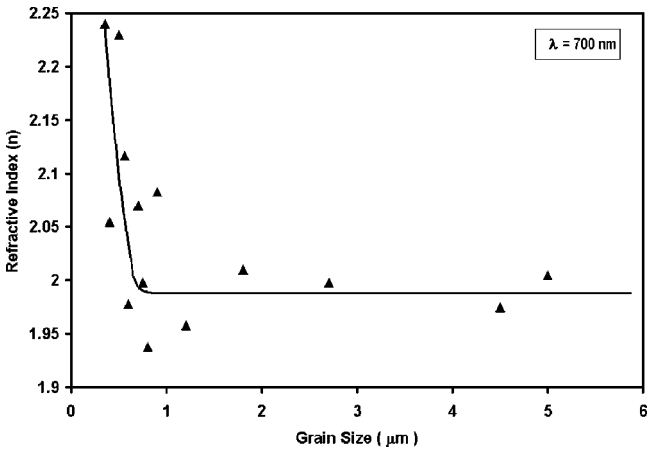

FIG. 8. The overall variation of refractive index n (determined at $\lambda = 700$ nm) with grain size (the combined data from all the three experiments).

The refractive index determined here may be treated as an ordinary refractive index because of the well-oriented (hh0) parallel to the substrate. The ordinary refractive indexes of a CdI_2 crystal were determined to be 2.36,[4] 2.4,[29] 2.35,[30] and 2.38 (Ref. 31) at a wavelength of 700 nm. In the present study, the ordinary refractive index determined at the same wavelength (700 nm) varies for samples studied by the three different experiments. In any case the maximum is $n = 2.25$ and the minimum is $n = 1.95$. Even the maximum value of n of the present study is less than the single-crystal average value reported earlier by about 0.12. The main reason for the difference is the polycrystalline nature of the films as opposed to the single crystals. In a polycrystalline sample the packing density of crystalline grains would dictate n, and the packing density depends on the grain size and their alignments, etc. Therefore, a slightly smaller refractive index may be expected for a polycrystalline sample as compared to single crystals. In fact, we have tried to see such a possibility by plotting the combined data of n from the three experiments as a function of grain size in Fig. 8. We can see an initial sharp fall and a subsequent saturation in the figure. The SEM results showed (Fig. 3) a dense packing for smaller uniform grains and a decreasing packing density with flattening and nonuniformally growing grains, creating voids. Therefore, the observed variation of the refractive index as a function of three experimental parameters could be mainly due to the packing density of grains in the sample, consistent with SEM results. Finally, the effect of residual stress on n may not be significant and cannot be separated from the effect of the packing density. The effect of a hydrostatic pressure of about 6.9×10^9 N/m^2 at 300 K on ZnTe film produced a mere decrease of 0.06 in $n = 2.91$ measured at 700 nm.[32] Therefore, a much larger variation of about 0.3 in n of the present study is dictated by the packing density of grains as revealed by SEM.

IV. CONCLUSIONS

The vacuum-evaporated stoichiometric CdI_2 films grown at very low deposition rates show a 4H polytype with a well-oriented (hh0) parallel to the substrate plane having a residual tensile stress perpendicular to these planes. The effects of the film thickness and heat treatment temperature on structural (residual stress) and optical (E_g) properties are similar and significant. The effect of the substrate temperature is nominal and opposite as compared to other two above-mentioned effects. Almost the same magnitude of threshold residual stress has been observed in grain size and E_g dependencies. The flattening and increasing grain size along the film length could be a manifestation of the intergranular tensile microstress that balances the tensile stress along the thickness up to a certain limit beyond which the film cracks. The decrease of E_g linearly with stress above the threshold may be assigned to a modification of the valence-band structure (I $5p$ character) due to the fractional increase in I-I distance. However, the existence of a threshold stress is not quite clear and may be due to the polytypism of CdI_2. The behavior of the refractive index with grain size seems to be quite consistent with the behavior of the packing density of crystallites with grain size, as seen by SEM. We hope these results are interesting enough to provide a further understanding of layered compounds and polytypism.

ACKNOWLEDGMENTS

We would like to thank P. Arun, Vinod Kumar Paliwal, Ashutosh Bharadwaj, Kirti Ranjan, Naveen Gaur, Rajeevi, and Hina for their helpful discussions and P.C. Padmakshan, Department of Geology, University of Delhi, for carrying out x-ray diffraction measurements. The help of Dr. N.C. Mehra, USIC, Delhi University in the measurements of EDAX and SEM is gratefully acknowledged.

*Electronic address:pankaj_andc@indiatimes.com
†Electronic address: agni@physics.du.ac.in

[1] F. Hulliger, in *Structural Chemistry of Layer-Type Phases*, edited by F. Levy (Reidel, Dordrecht, 1976), pp. 31–34 and 275.
[2] G.C. Trigunayat, Solid State Ionics **48**, 3 (1991).
[3] D.L. Greenaway and R. Nitsche, J. Phys. Chem. Solids **26**, 1445 (1965).
[4] P.A. Lee, G. Said, R. Davis, and T.H. Lim, J. Phys. Chem. Solids **30**, 2719 (1969).
[5] Y. Takemura, T. Komatsu, and Y. Kaifu, Phys. Status Solidi B **72**, K87 (1975).
[6] J.V. McCanny, R.H. Williams, R.B. Murray, and P.C. Kemeny, J. Phys. C **10**, 4255 (1977).
[7] J. Bordas, J. Robertson, and A. Jakobsson, J. Phys. C **11**, 2607 (1978).
[8] J. Robertson, J. Phys. C **12**, 4753 (1979).
[9] R. Coehoorn, G.A. Sawatzky, C. Haas, and R.A. deGroot, Phys. Rev. B **31**, 6739 (1985).
[10] I. Pollini, J. Thomas, R. Coehoorn, and C. Hass, Phys. Rev. B **33**, 5747 (1986).
[11] R.D. Bringans and W.Y. Liang, J. Phys. C **14**, 1065 (1981).
[12] R.M. Yu, Philos. Mag. **16**, 1167 (1967).

[13] S. Brahms, Phys. Lett. **19**, 272 (1965).
[14] S. Kondo, S. Matasuoka, and T. Saito, Phys. Status Solidi B **186**, K77 (1994).
[15] S. Kondo, S. Matasuoka, and T. Saito, Phys. Status Solidi A **165**, 271 (1998).
[16] H. Nakagawa, T. Yamada, H. Matsumoto, and T. Hayashi, J. Phys. Soc. Jpn. **56**, 1185 (1987).
[17] P. Tyagi, A.G. Vedeshwar, and N.C. Mehra, Physica B **304**, 166 (2001).
[18] S. Kondo, T. Suzuki, and T. Saito, J. Phys. D **31**, 2733 (1998).
[19] L.I. Maissel and R. Glang, in *Handbook of Thin Film Technology* (McGrawHill, New York, 1970). P. 9-8.
[20] B.D. Cullity, *Elements of X-ray Diffraction*, 2nd ed. (Addison-Wesley, Redwood City, California, 1978), p. 102.
[21] D. Dye, H.J. Stone, and R.C. Reed, Curr. Opin. Solid State Mater. Sci. **5**, 31 (2001).
[22] M. Ohring, *The Material Science of Thin Films* (Academic Press, San Diego, 1992).
[23] A.E. Ennos, Appl. Opt. **5**, 51 (1966).
[24] N.F. Mott and E.A. Davis, *Electronic Processes in Non-crystalline Materials* (Clarendon Press, Oxford, 1979), pp. 273 and 274.
[25] R. Bacewicz, B. Palosz, and S. Gierlotka, Phys. Status Solidi B **130**, K135 (1985).
[26] *Semiconductors–Basic Data*, 2nd ed., edited by O. Madelung (Springer-Verlag, Berlin, 1996), p. 188.
[27] A.D. Brothers and J.T. Pajor, Phys. Rev. B **14**, 4570 (1976).
[28] R. Swanepoel, J. Phys. E **16**, 1214 (1983).
[29] M.R. Tubbs, J. Phys. Chem. Solids **27**, 1667 (1966).
[30] S. Kondo and H. Matsumoto, J. Phys. Soc. Jpn. **50**, 3047 (1981).
[31] M.R. Tubbs, J. Phys. Chem. Solids **30**, 2323 (1969).
[32] M. Lindner, G.F. Schotz, P. Link, H.P. Wagner, W. Kuhn, and W. Gebhardt, J. Phys.: Condens. Matter **4**, 6401 (1992).